Bull. Chem. Soc. Ethiop. **2024**, 38(4), 877-887. ISSN 1011-3924
Printed in Ethiopia
Online ISSN 1726-801X
DOI: https://dx.doi.org/10.4314/bcse.v38i4.5

N-LIGANDS MEDIATED Co(II) COORDINATION POLYMER INCORPORATING 5-HYDROXYISOPHTHALIC ACID: SYNTHESES, STRUCTURES, AND THEORETICAL CALCULATIONS

J.D. Feng[1,2], Y.Z. Song[1,2], X.Y. Wang[1,2*], Y. Song[1,2], Y. Yu[2] and J. X. Liu[1,2]

[1]Key Laboratory of Preparation and Applications of Environmental Friendly
Materials, Jilin Normal University, Ministry of Education, Changchun 130103, China
[2]Department of Chemistry, Jilin Normal University, Siping 136000, China

(Received October 13, 2023; Revised January 30, 2024; Accepted February 2, 2024)

ABSTRACT. The coordination polymer, $[Co(L)(hip)]_n$ (**1**), (L = 11-fluoro-pyridine[3,2-a:2',3'-c]phenazine and H_2hip = 5-hydroxyisophthalic acid), has been successfully synthesized under hydrothermal condition. Complex **1** crystallizes in tetragonal, space group *P4₃2₁2* and the asymmetric unit consists of one Co(II) ion, one hip^{2-} anion and one ligand L. The binuclear $[Co_2(L)_2(hip)_4]^{4-}$ second building unit is formed by the coordination of four different hip^{2-} anions and two Co(L) moieties. The adjacent Co(II) centers are connected by the bridging hip^{2-} anions to form a one-dimensional helical chain. Finally, a three-dimensional structure is formed by the self-assembly of the coordination bond between the Co centers and the hip^{2-} anions. The powder X-ray diffraction, thermal analysis, IR analysis, UV-Vis absorption spectrum, photoluminescent properties and theoretical calculation for complex **1** are straight displayed.

KEY WORDS: Co(II), 5-hydroxyisophthalic acid, Coordination polymer, Crystal structure

INTRODUCTION

Metal coordination polymers (CPs) are a promising class of crystalline porous materials composed of metal-containing nodes and organic ligands. Due to their intriguing topology, easy-to-functionalize surface structure, and properties in gas storage and separation, ion exchange, sensing luminescence, etc., CPs have drawn a lot of attention in recent decades [1-12]. The structure diversity of CPs and their chemical properties are almost limitless on the basis of the properties of metal ions and their coordination modes with various organic ligands. Especially, the nature of the organic ligand and the synthetic strategy are the key factors in the synthesis of coordination polymer with predicted structures. Up to now, N-donor ligands with excellent coordination properties and multidentate carboxylate ligands with various configurations and coordination modes have been widely employed to construct CPs due to them coordinating to the metal centers in monodentate, bidentate, or bridging modes [13-16]. Among poly-carboxylate ligands, the best studied are dicarboxylates, tricarboxylates, and V-shaped aromatic dicarboxylates such as biphenyldicarboxylate [17, 18]. On the one hand, di- and polycarboxylates with flexible aliphatic backbones are expected to adopt various conformational freedoms [19, 21]. In addition, due to their coordination modalities, carboxylates are also anticipated to have a significant role in mediating molecular-molecular interaction, electron transport, magnetic exchange channels and biological uses [22]. For example, the V-shaped aromatic dicarboxylate, 5-hydroxyisophthalic acid ligand (H_2hip), as a multidentate O-donor ligand was used to coordinate and self-assemble into a 3D supramolecular structure with Cd(II) metal and nitrogen-containing ligands in 2021 [23].

Based on the above, towards the goal of designing novel materials, we selected the H_2hip as the linker and 11-fluoro-pyridine[3,2-a:2',3'-c]phenazine ligand (L) as a N-donor chelating ligand, generating a new coordination polymer, namely $[Co(L)(hip)]_n$ (**1**). The powder X-ray diffraction,

---

*Corresponding author. E-mail: wangxiuyanjlnu2004@163.com thermal analysis, UV-Vis absorption spectrum and fluorescent behaviors of complex **1** have been investigated.

EXPERIMENTAL

Materials and measurements

All reagents were of analytical reagent grade and used as received without further purification. Elemental analysis was carried out with a Perkin-Elmer 240C analyzer. The powder X-ray diffraction (PXRD) patterns of the samples were recorded on a Rigaku Dmax 2000 X-ray diffractometer with graphite monochromatized Cu*Kα* radiation ($\lambda = 0.154$ nm). Thermal stability experiment was performed on a TG SDT2960 thermal analyzer from 24 to 900 °C under a nitrogen gas. IR spectrum was recorded in the range of 4000-400 cm^{-1} on a Perkin-Elmer Spectrum One FTIR spectrometer using a KBr pellet. UV-Vis absorption spectrum was collected on a finely ground sample with a Shimadzu UV-2550 visible-ultraviolet spectrophotometer. The emission spectra were carried out on a Renishaw inVia Raman Microscope.

A single crystal was chosen and mounted on a Bruker-AXS Smart CCD diffractometer equipped with a graphite-monochromatized MoKα ($\lambda = 0.71073$ Å) radiation by using an ω-ϕ scan method at 298(2) K. The structure was solved by direct methods with SIR2014 [24] and refined with SHELXL2018/3 [25] programs by full-matrix least-squares techniques on F^2. All H atoms were found by generated calculations with refining as riding, and the non-hydrogen atoms were refined with anisotropic temperature parameters. The X-ray crystallographic and refinement parameters are given in Table 1.

Table 1. Crystalline data and refinement parameters for complex **1**.

Formula	$C_{26}H_{12}CoFN_4O_5$
M_r (g.mol^{-1})	538.33
Crystal system	Tetragonal
Space group	$P4_32_12$
a, b, c [Å]	11.7044(17), 11.7044(17), 31.497(6)
α, β, γ (°)	90, 90, 90
V (Å^3)	4314.9(15)
Z	8
ρ (g.cm^{-3})	1.657
μ (mm^{-1})	0.855
F(000)	2176
Crystal size (mm)	0.23 × 0.21 × 0.15
Temperature (K)	298(2)
Mo *Kα* radiation, λ (Å)	0.71073
θ (min-max) (°)	3.118, 24.999
Data set	$-13\leq h\leq 13$; $-13\leq k\leq 11$; $-37\leq l\leq 37$
Tot., Unique data, R_{int}	28653, 3791, 0.0882
Observed [I>2σ(I)] reflections	3487
Nreflections, Nparameters	3791, 347
$R[F^2>2\sigma(F^2)]$, $wR(F^2)$, S	0.0561, 0.1267, 1.080
$\Delta\rho_{min}$, $\Delta\rho_{max}$ (e.Å^{-3})	-0.375, 0.571

Synthesis of ligand L

A mixture of 1,2-diamino-4-fluorobenzene (20 mmol, 2.52 g), 1,10-phenanthroline-5,6-dione (20 mmol, 4.20 g) and acetic acid (0.2 mL) in 40 mL ethanol was added to a three neck bottle and refluxed for 6 h. Then cooled to room temperature, pale yellow precipitation can be obtained, and the precipitation can be washed with water ethanol and collected by vacuum suction filtration (Scheme 1). Yield: 61% based on 1,10-phenanthroline-5,6-dione.

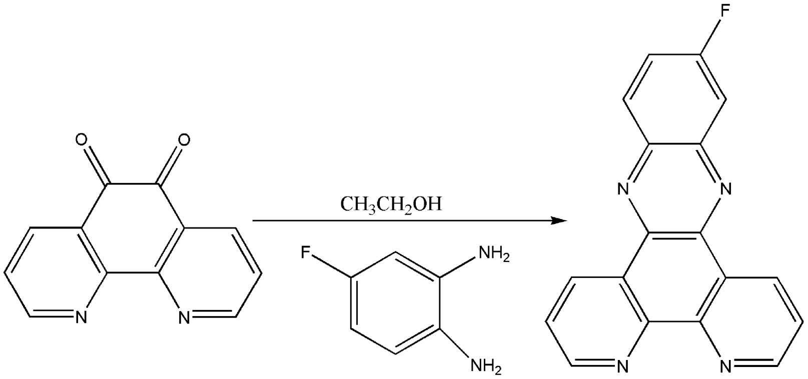

Scheme 1. The synthesis of ligand L.

Synthesis of [Co(L)(hip)]$_n$ (1)

A reaction mixture of $Co(NO_3)_2{\cdot}6H_2O$ (0.3 mmol, 0.090 g), H_2hip (0.3 mmol, 0.055 g), L (0.15 mmol, 0.045 g), 3 mL anhydrous ethanol and H_2O (7 mL) had its pH value adjusted to 3.66 with 1 $mol{\cdot}L^{-1}$ NaOH solution. The mixture was then stirred for 20 min in air and sealed in a 16 mL Teflon^{TM}-lined autoclave, which was heated to 468 K for 72 h, followed by slow cooling (5 $K{\cdot}h^{-1}$). The resulting rhomboid crystals were washed with distilled water and dried in air (yield: ca. 32%). Anal. calcd. for $C_{26}H_{12}CoFN_4O_5$ (FW 538.33): C, 58.01; H, 2.25; N, 10.41. Found: C, 57.36; H, 2.21; N, 10.28.

RESULTS AND DISCUSSION

Powder X-ray Diffraction

The powder X-ray diffraction (PXRD) patterns of the samples were recorded on a Rigaku Dmax 2000 X-ray diffractometer with graphite monochromatized CuKα radiation ($\lambda = 0.154$ nm) in the 2θ angle range from 5 to 50°. The powder X-ray diffraction (PXRD) results indicate that the reflection peaks are in good agreement with the corresponding simulated ones, indicates that the complex **1** is pure phase (Figure 1). The differences in peak strength perhaps by the preferred direction of the powder samples.

Thermogravimetric analyses

Thermal stability experiment was performed on a TG SDT2960 thermal analyzer from 24 to 900 °C under a nitrogen gas with a heating rate of 10 °C min^{-1}. The anhydrous complex **1** remain steady around 271 °C, then begins to decompose and ends above 683 °C (Figure 2a). The weight loss is attributed to both the N-containing ligand and the organic group $C_8H_4O_4$ of hip^{2-} anions (obsd. 85.9%, calcd. 86.1%). However, it is difficult to determine these weight losses accurately as these processes are overlapped with the weight losses due to the dissociation of the organic fractions from the anhydrous crystal. The remaining weight of obsd.14.1% corresponds to calcd. 13.9% of Co and O components, demonstrating that the end-product is CoO. The thermogravimetric analyses indicate that the thermostability of complex **1** is relatively good [26].

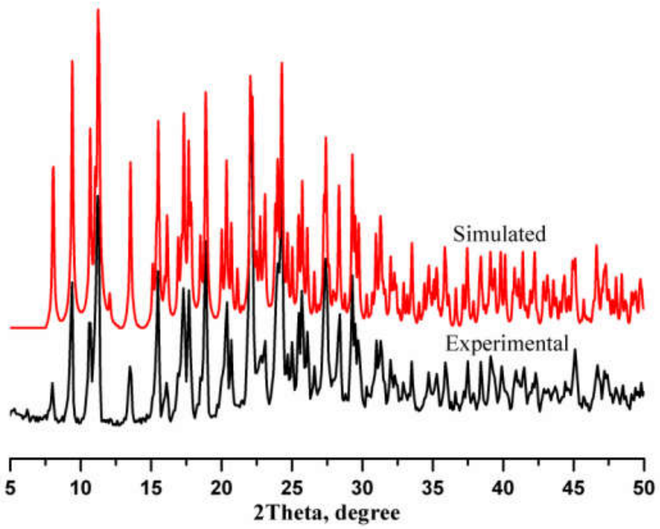

Figure 1. Experimental and simulated PXRD patterns of complex **1**.

IR analysis

The solid-state IR spectrum of **1** was illustrated in the region of 4000-400 cm^{-1} (Figure 2b). The strong and wide peak at 3431 cm^{-1} was observed, which is characteristic of the stretching vibrations of N–H bond of ligand L. The strong peaks at 1404 and 1611 cm^{-1} could be ascribed to the asymmetric and symmetric vibrations of carboxylate groups of the hip^{2-} anions. The separations between $\nu_{as}(COO^-)$ and $\nu_s(COO^-)$ are 207 cm^{-1} for **1**, respectively [27]. The C–N and C=N stretching vibrations of ligand L were observed at 1137 and 1440 cm^{-1}.

Ultraviolet-visible spectroscopy

At room temperature, the solid UV-Vis absorption spectrum of **1** was carried out in the wavelength range of 200-700 nm with the barium sulfate as the background during scanning (Figure 3a). The broad intense absorption peak of **1** is observed at 350-460 nm, which can be ascribed to π-π* or n-π* transitions of the aromatic rings [28].

Photoluminescent spectra

In this work, solid-state luminescent properties were performed for **1**, H_2hip and ligand L (Figure 3b). The main emission peaks of H_2hip and L are at 377 and 492 nm (λ_{ex} = 325 nm), respectively. These emissions of the free ligands are probably attributable to the $\pi^* \rightarrow n$ or $\pi^* \rightarrow \pi$ transitions [29]. The emission peak of **1** occurs at 520 nm (λ_{ex} = 325 nm). Compared with the free ligand L, the emission peak of **1** is red-shifted by 28 nm. The emission of **1** is neither ligand-to-metal charge transfer (LMCT) nor metal-to-ligand charge transfer (MLCT). The emission of **1** can probably be attributed to the intraligand transitions [30].

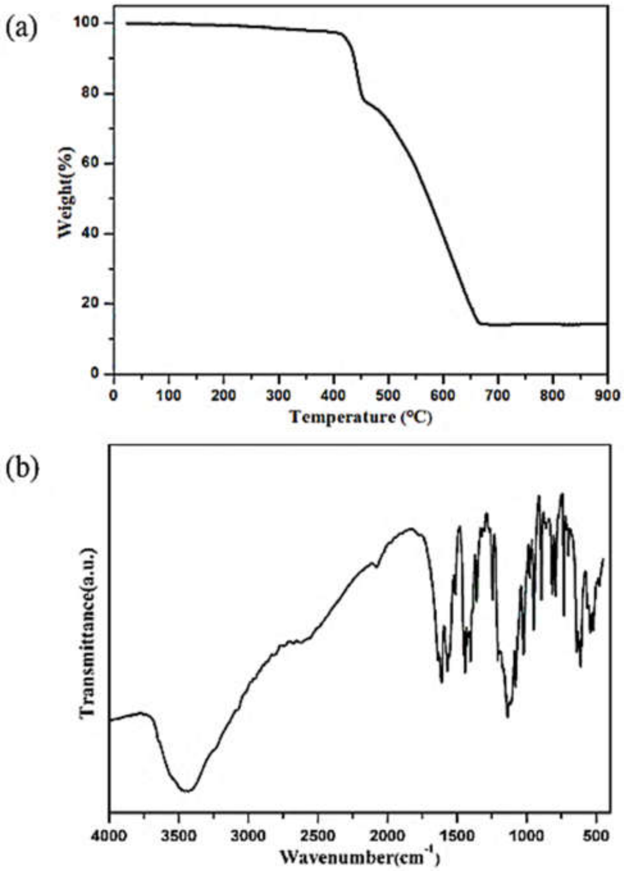

Figure 2. (a) View of the thermogravimetric analyses curve of complex **1**; (b) IR spectrum of complex **1**.

Theoretical calculations

In this work, all calculations were performed on the Gaussian09 program [31] with the parameters of the molecular structure from the experimental data of **1**. Natural bond orbital (NBO) analysis [32] was carried out by density functional theory with the B3LYP hybrid functional [33], and functional and the LANL2DZ basis set [34].

The selected natural atomic charges and natural electron configuration for **1** are shown in Table 2. It signals that the electronic configurations of Co(II) ion, O and N atoms are $4s^{0.29}3d^{6.39}4p^{0.38}4d^{0.01}$, $2s^{1.65,1.67}2p^{5.19\sim5.22}3p^{0.01}$ and $2s^{1.33}2p^{4.27,4.28}3p^{0.02}$, respectively. According to the above results, one can confirm that the Co(II) ion coordination with O and N atoms is mostly on the 4*s*, 3*d* and 4*p* orbitals. O and N atoms supply electrons of 2*s*, 2*p* and 3*p* to the Co(II) ion and generate coordination bonds. Hence, according to valence-bond theory the atomic net charge distribution in the complex indicates obvious covalent interactions between the coordinated atoms and Co(II) ion.

The energies of HOMO and LUMO for complex **1** are acquired as −4.73 and −3.77 eV respectively. As can be seen from Figure 4, the HOMO and HOMO−1 are mainly composed of the *d* orbital of Co(II) ion, *p* orbitals of three O and two N atoms coordinated with Co(II) ion. The LUMO and LUMO+3 are mostly consisted of the π orbital of the hip^{2-} anions. The HOMO–2, HOMO–3, LUMO+1 and LUMO+2 are mainly including the orbital of the L and hip^{2-} anions.

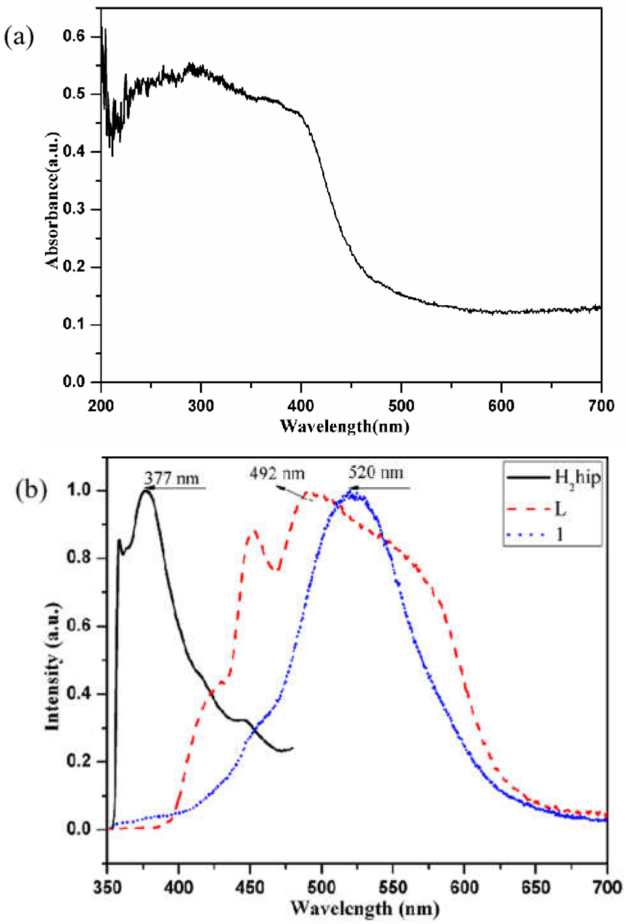

Figure 3. (a) UV-Vis absorption spectra of **1**; (b) solid-state photoluminescent spectra of H_2hip, L and **1** at room temperature.

Table 2. Selected natural atomic charges and natural electron configuration of **1**.

Atom	Net charge	Electron configuration
Co(1)	1.872	[core]4*s*(0.29)3*d*(6.39)4*p*(0.38)4*d*(0.01)
O(1)	-0.862	[core]2*s*(1.67)2*p*(5.19)3*p*(0.01)
O(3)^{i}	-0.935	[core]2*s*(1.65)2*p*(5.28)3*p*(0.01)
O(4)^{ii}	-0.889	[core]2*s*(1.67)2*p*(5.22)3*p*(0.01)
N(1)	-0.952	[core]2*s*(1.33)2*p*(4.27)3*p*(0.02)
N(2)	-0.970	[core]2*s*(1.33)2*p*(4.28)3*p*(0.02)

Symmetry transformation: (i) *x*+1/2, -*y*+1/2, -*z*+5/4; (ii) *x*+1/2, -*y*+1/2, *z*-1/4.

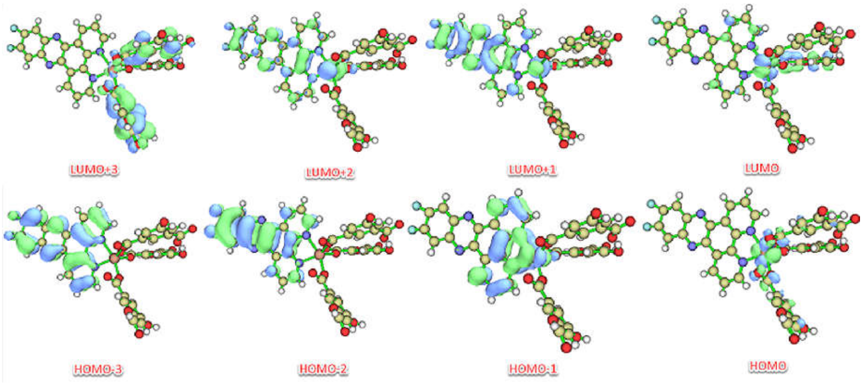

Figure 4. Frontier molecular orbitals of **1**.

Crystal structure

The asymmetric unit of complex **1** consists of one crystallographically unique Co cation, one hip^{2-} anion and one ligand L. As shown in Figure 5a, the Co(II) ion is located in a distorted quadrangular pyramidal coordination geometry, equatorially coordinated by two carboxylate atoms O3^{i} and O4^{ii} [the symmetry codes for **1** are given in Table 3] from two different hip^{2-} anions, two pyridine N atoms [N1 and N2] from one ligand L. At the apical position is carboxylate atom O1 from another hip^{2-} anions. The maximum and minimum bond angles for Co^{2+} ion are 155.5(3) and 75.4(2)°, respectively, with an average value of 106.54(3)°, which slightly deviates from the angle of 109.34° in a perfect tetrahedron. The Co-O and Co-N bond lengths vary from 1.949(5) to 2.163(7) Å, and more detailed selected bond distances and bond angles are listed in Table 3. In Figure 5b, four N atoms (N1, N2 and N1^{v}, N2^{v}) of two ligands L adopt a chelating μ_1-η^1: η^1 mode to link the adjacent Co atoms, then two Co(L) moieties are linked by four different hip^{2-} anions to form a binuclear $[Co_2(L)_2(hip)_4]^{4-}$ second building unit (SBU). It is interesting to note that the carboxylate oxygen atoms of the hip^{2-} anions are all deprotonated and take different bridging patterns. The first carboxylate group (O1 and O1^{v}) of two different hip^{2-} anions show a monodentate coordination mode to link one Co center of the adjacent SBU. The second carboxylate group (O3^{iii}, O4^{iii} and O3^{iv}, O4^{iv}) of two different hip^{2-} anions exhibit a bridging bidentate coordination to connect two adjacent Co centers. The bridging hip^{2-} anions link neighboring dinuclear Co(II) clusters to yield a 1D left-handed helical chain along the c-axis (Figure 5c). The existence of these helical chains and the coordination bond between the Co centers and the hip^{2-} anions promote the self-assembly of the three-dimensional structure (Figure 6).

Table 3. Selected bond distances (Å) and bond angles (°) for **1**

Bond lengths (Å)		Bond angles (°)	
O(3)–Co(1)^{i}	2.019(6)	O(1)–Co(1)–O(4)^{iii}	97.6(2)
O(4)–Co(1)^{ii}	2.013(5)	O(1)–Co(1)–O(3)^{iv}	94.3(2)
O(1)–Co(1)	1.949(5)	O(4)^{iii}–Co(1)–O(3)^{iv}	95.0(3)
N(1)–Co(1)	2.163(7)	O(1)–Co(1)–N(2)	119.0(3)
N(2)–Co(1)	2.148(7)	O(4)^{iii}–Co(1)–N(2)	90.2(2)
		O(3)^{iv}–Co(1)–N(2)	145.3(3)
		O(1)–Co(1)–N(1)	106.6(3)
		O(4)^{iii}–Co(1)–N(1)	155.5(3)
		O(3)^{iv}–Co(1)–N(1)	86.5(3)
		N(2)–Co(1)–N(1)	75.4(2)

Symmetry transformations used to generate equivalent atoms: (i) x+1/2, -y+1/2, -z+5/4, (ii) -y+1/2, x+1/2, z-1/4, (iii) y-1/2, -x+1/2, z+1/4, (iv) x-1/2, -y+1/2, -z+5/4.

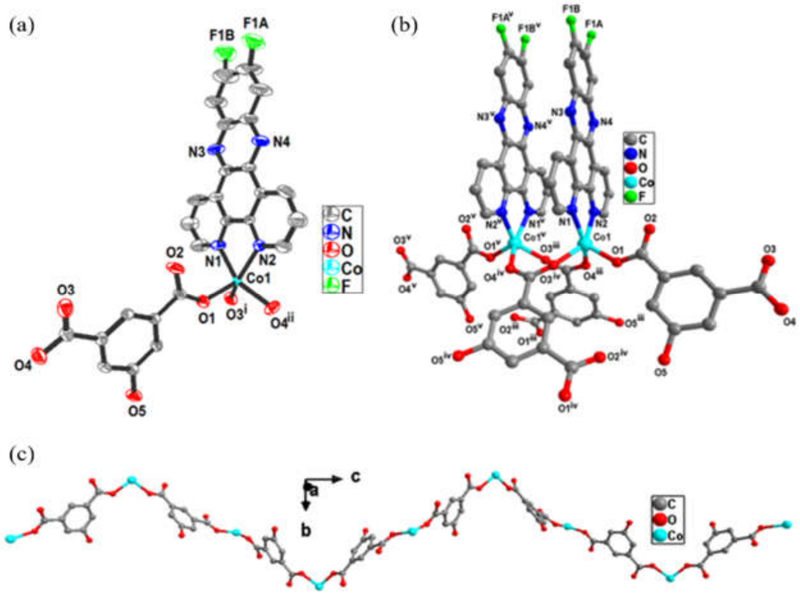

Figure 5. (a) Coordination environment of the complex **1** is showing. Displacement ellipsoids at the 30% probability level; (b) The $[Co_2(L)_2(hip)_4]^{4-}$ second building unit assembled by four hip^{2-} anions, two L and two Co(II) ions; (c) View of the one-dimensional chain structure of complex **1**. (Symmetry transformations used to generate equivalent atoms: (i) *x*+1/2, -*y*+1/2, -*z*+5/4, (ii) -*y*+1/2, *x*+1/2, *z*-1/4, (iii) *y*-1/2, -*x*+1/2, *z*+1/4, (iv) *x*-1/2, -*y*+1/2, -*z*+5/4.)

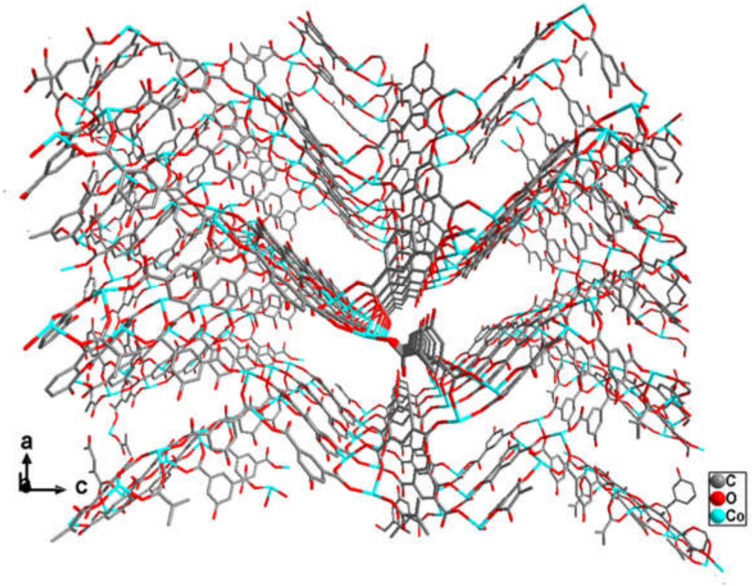

Figure 6. View of the 3D metal-organic framework (ligands L were omitted for clarity).

CONCLUSION

In summary, we have developed a synthetic strategy toward 3D coordination frameworks $[Co(L)(hip)]_n$ by using a V-shaped dicarboxylate ligand, a ligand L and a transition metal Co(II) ion. In complex **1**, the four N atoms of the ligand L adopt a chelating μ_1-η^1: η^1 mode to link adjacent Co atoms, and different hip^{2-} anions link the two Co(L) moieties to form a binuclear SBU: $[Co_2(L)_2(hip)_4]^{4-}$. The carboxylic acid groups of the hip^{2-} anions use monodentate and bidentate coordination modes to connect adjacent binuclear Co(II) clusters, respectively, to generate a 1D left-handed helical chain along the c-axis. The 3D structure is then self-assembled through the coordination bond between the metal and hip^{2-} anions. In addition, complex **1** exhibits thermal stabilities and photoluminescent properties in the solid state.

ACKNOWLEGDEMENTS

The authors are thankful for the Science and Technology Research Project from the Education Department of Jilin Province (No. JJKH20170373KJ).

SUPPLEMENTARY DATA

Crystallographic data have been deposited with the Cambridge Crystallographic Data Centre as supplementary publication number CCDC 2131751. Copies of this information may be obtained free of charge from The Director, CCDC, 12 Union Road, Cambridge, CB2 1EZ, UK (fax: +44-1223-336033; email: deposit@ccdc.cam.ac.uk or www: http://www.ccdc.cam.ac.uk).

REFERENCES

1. Yang, Y.M.; Feng, C.; Jiang, Y.H.; Du, D.H.; Zhao, H.; Zhang, G.N.; Wang, Y.C.; Zhao, Q. Synthesis, crystal structure, Hirshfeld surface analysis and electrochemiluminescence property of A 2D Ag(I) coordination polymer. *J. Mol. Struct*. **2023**, 1292, 136145.
2. Song, Y.; Fu, T.X.; Ning, J.B.; Wang, X.Y.; Liu, J.X.; Chang, L.M. Syntheses, structure and characterization of a new Pb(II) coordination polymer based on 1,10-phenanthroline derivative and 5-hydroxyisophthalic acid. *J. Cluster Sci.* **2023**, 1-7. DOI: http://dx.doi.org/10.2139/ssrn.4380101
3. Ahmed, D.S.; El-Hiti, G.A.; Yousif, E.; Ali, A.A.; Hameed, A.S. Design and synthesis of porous polymeric materials and their applications in gas capture and storage: a review. *J. Polym. Res*. **2018**, 25, 1-21.
4. Lawson, S.; Newport, K.; Pederniera, N.; Rownaghi, A.A.; Rezaei, F. Curcumin delivery on metal-organic frameworks: The effect of the metal center on pharmacokinetics within the M-MOF-74 family. *ACS Appl. Bio Mater*. **2021**, 4, 3423-3432.
5. Ai, J.; Yang, L.; Tian, Z.Z. Cobalt(II) and nickel(II) complexes based on 2,5-di (pyridine-4-yl) thiazolo[5,4-d]thiazole and dicarboxylate ligands: Synthesis, structures and properties. *Z Naturforsch B* **2023**, 78, 331-337.
6. Rosa, P.P.F.; Kitagawa, Y.; Hasegawa, Y. Luminescent lanthanide complex with seven-coordination geometry. *Coord. Chem. Rev.* **2020**, 406, 213153.
7. Dadashi, J.; Khaleghian, M.; Hanifehpour, Y.; Mirtamizdoust, B.; Joo, S.W. Lead(II)-azido metal-organic coordination polymers: Synthesis, structure and application in PbO nanomaterials preparation. *Nanomaterials* **2022**, 12, 2257.

8. Shi, X.X.; Qu, X.J.; Chai, J.; Tong, C.X.; Fan, Y.; Wang, L. Stable coordination polymers with linear dependence color tuning and luminescent properties for detection of metal ions and explosives. *Dyes Pigments* **2019**, 170, 107583.
9. Qiao, W.; Waseem, I.; Shang, G.M.; Wang, D.; Li, Y.W.; Besenbacher, F.; Niemantsverdriet, H.; Yan, C.L.; Su, R. Paired electrochemical N-N coupling employing a surface-hydroxylated Ni_3Fe-MOF-OH bifunctional electrocatalyst with enhanced adsorption of nitroarenes and anilines. *ACS Catal*. **2021**, 11, 13510-13518.
10. Karmakar, A.; Paul, A.; Santos, P.M.R.; Santos, I.R.M.; da Silva, M.F.C.G.; Pombeiro, A.J.L. Novel anthracene and pyrene containing Cd (II)-based coordination polymers for adsorptive removal of toxic dyes from aqueous medium. *Colloid Surface A*. **2023**, 670, 131488.
11. Wang, Z.Y.; Liu, T.; Jiang, L.P.; Asif, M.; Qiu, X.Y.; Yu, Y.; Xiao, F.; Liu, H.F. Assembling metal-organic frameworks into the fractal scale for sweat sensing. *ACS Appl. Mater. Interfaces*. **2019**, 11, 32310-32319.
12. Song, Y.; Xu, L.P.; Li, G.T.; Wang, X.Y. A 3D supramolecular polymer involving hydrogen bonds based on nickel(II), 1, 3-benzenedicarboxylic acid, and a nitrogen-containing ligand. *J. Struct. Chem.* **2021**, 62, 1105-1111.
13. Madanhire, T.; Van Brecht, B.; Abrahams, A. Synthesis and crystal structure of a mixed-ligand zinc(II) complex derived from ethyl (2, 6-dimethylphenylcarbamoyl) formate and 1, 10-phenanthroline. *Bull. Chem. Soc. Ethiop*. **2023**, 37, 891-900.
14. Feng, J.D.; Li, Z.R.; Wang, X.Y. Two novel lead(II) coordination complexes incorporating phenanthroline derivate: synthesis and characterization. *Main Group Met. Chem.* **2023**, 46, 20228045.
15. Berezhnytska, O.S.; Savchenko, I.O.; Horbenko, A.E.; Rohovtsov, O.O.; Rusakova, N.V.; Trunova, O.K. Synthesis, structure of luminescence complexes and metalopolymers of Dy(III) and influence of the nature of substitutes on their emission. *J. Mol. Struct*. **2023**, 1293, 136148.
16. Vlasyuk, D.; Łyszczek, R.; Mazur, L.; Pladzyk, A.; Hnatejko, Z.; Woźny, P. A series of novel 3D coordination polymers based on the quinoline-2,4-dicarboxylate building block and lanthanide(III) ions—temperature dependence investigations. *Molecules* **2023**, 28, 6360.
17. Shi, Y.; Song, M.M.; Tao, D.L.; Bo, Q.B. Two novel 2D Zn(II) coordination polymers with quinoline-3-carboxylic acid and tetraphenylphthalic acid: Synthesis and photoluminescence properties. *J. Chem. Crystallogr.* **2020**, 50, 198-205.
18. Pan, Z.R.; Shi, X.R.; Zheng, B.; Wang, X.F.; Fu, X.Q.; Liu, S.X.; Lang, L.M.; Liu, G.X. A unique 6-connected three dimensional cobalt(II) coordination compound: Preparation, structure and magnetic properties. *Inorg. Chem. Commun.* **2020**, 112, 107732.
19. Vakil, F.; Mantasha, I.; Shahid, M.; Ahmad, M. A dinuclear paddle-wheel Cu(II) complex $[Cu_2(L)_4(H_2O)_2]\cdot 2H_2O$ [HL = 2-(methoxycarbonyl) benzoic acid)]: Crystallographic, magnetic, and theoretical analyses. *J. Struct. Chem.* **2019**, 60, 1971-1982.
20. Sahoo1, P.K.; Biswal, S.K.; Azam, M. Transition metal complexes produced from dipicolinic acid: Synthesis, structural characterization, and anti-microbial investigations. *Bull. Chem. Soc. Ethiop*. **2022**, 36, 607-615.
21. Kaim, W.; Rall, J. Copper—a “modern” bioelement. *Angew. Chem. Int. Ed. Engl.* **1996**, 35, 43-60.
22. Su, B.H.; Shi, Y.H.; Peng, X.H.; Kong, Z.G.; Chang, L.M. A new cadmium(II) coordination polymer with 1,4-cyclohexanedicarboxylate acid and phenanthroline derivate: Synthesis and crystal structure. *Main Group Met. Chem*. **2022**, 45, 208-212.
23. Zeng, N.N.; Han, C.; Fu, L.S.; Cui, G.H. Two new ternary Cd(II) coordination polymers containing bis (thiabendazole) ligands as luminescent sensors for benzaldehyde and MnO_4^- anions. *J. Inorg. Organomet. Polym. Mater.* **2021**, 31, 4523-4531.
24. Burla, M.C.; Caliandro, R.; Carrozzini, B.; Cascarano, G.L.; Cuocci, C.; Giacovazzo, C.; Mallamo, M.; Mazzone, A.; Polidori, G. Crystal structure determination and refinement via SIR2014. *J. Appl. Crystallogr*. **2015**, 48, 306-309.

25. Sheldrick, G.M. Crystal structure refinement with SHELXL. *Acta Cryst.* **2015**, C71, 3-8.
26. Li, J.; Liu, Z.; Liu, Y.Y.; Liu, J.; Li, Y.Y.; Qiao, X.Y.; Huang, W.M.; Niu, Y.Y. POM-based metal-organic compounds: Assembly, structures and properties. *Main Group Chem.* **2021**, 20, 575-592.
27. Wen, Y.H.; Chen, C.G.; Wen, H.L.; Mu, X.W.; Yao, K. Syntheses, crystal structures, and fluorescent properties of two mixed-ligand cadmium coordination polymers based on dicarboxylate and bis-benzimidazole ligands. *J. Chem. Crystallogr.* **2018**, 48, 12-218.
28. Wang, J.F.; Feng, T.; Li, Y.J.; Sun, Y.X.; Dong, W.K.; Ding, Y.J. Novel structurally characterized Co(II) metal-organic framework and Cd(II) coordination polymer self-assembled from a pyridine-terminal salamo-like ligand bearing various coordination modes. *J. Mol. Struct.* **2021**, 1231, 129950.
29. Mikheev, Y.A.; Ershov, Y.A. Assignment of the $\pi \rightarrow \pi^*$ and $n \rightarrow \pi^*$ transitions to the spectral bands of azobenzene and dimethylaminoazobenzene. *Russ. J. Phys. Chem.* **2018**, 92, 1499-1507.
30. Zhang, L.Y.; Liu, G.F.; Zheng, S.L.; Ye, B.H.; Zhang, X.M.; Chen, X.M. Helical ribbons of cadmium(II) and zinc(II) dicarboxylates with bipyridyl-like chelates - syntheses, crystal structures and photoluminescence. *Eur. J. Inorg. Chem.* **2003**, 16, 2965-2971.
31. Frisch, M.J.; Trucks, G.W.; Schlegel, H.B.; Scuseria, G.E.; Robb, M.A.; Cheeseman, J.R.; Fox, D.J. *Gaussian 09, rev.* Gaussian Inc: Wallingford; **2009**.
32. Reed, A.E.; Curtiss, L.A.; Weinhold, F. Intermolecular interactions from a natural bond orbital, donor-acceptor viewpoint. *Chem. Rev.* **1988**, 88(6), 899-926
33. Lee, C.; Yang, W.; Parr, R.G. Development of the Colle-Salvetti correlation-energy formula into a functional of the electron density. *Phys. Rev. B.* **1988**, 37, 785-789.
34. Dunning Jr, T.H.; Hay, P.J. *In Modern Theoretical Chemistry* Schaefer III, H.F. (Eds.), Plenum: New York; **1976**, 3, 1-28.